Pleistocene aragonite crust diagenesis mimics microbialite fabrics (Danakil Depression, Ethiopia)

David Jaramillo-Vogel [a,b,*], Juan Carlos Braga [c], Haileyesus Alemu Negga [a], Torsten Vennemann [d], Eva De Boever [a,1], Jean-Charles Schaegis [a], Valentin Rime [a], Balemwal Atnafu [e], Tesfaye Kidane [f], Anneleen Foubert [a]

[a] University of Fribourg, Department of Geosciences, Chemin Du Musée 6, Fribourg, Switzerland
[b] Particle Vision GmbH, Passage du Cardinal 13B, Fribourg, Switzerland
[c] Departamento de Estratigrafía y Paleontología, Universidad de Granada, Avenida de la Fuente Nueva 2, C.P., Granada, Spain
[d] Université de Lausanne, Institut des dynamiques de la surface terrestre, Géopolis, Lausanne, Switzerland
[e] School of Earth Sciences, Addis Ababa University, Addis Ababa, Ethiopia
[f] University of Kwazulu-Natal, School of Agricultural, Earth and Environmental Sciences, Westville Campus, Durban, South Africa

ARTICLE INFO

ABSTRACT

Fibrous aragonite crusts occur in two consecutive Pleistocene successions in the Danakil Depression (Afar, Ethiopia). Lateral transitions between pristine and altered fibrous aragonite crusts document changes in texture associated with diagenesis. Crusts formed as essentially abiotic seafloor precipitates at the transition from marine to evaporitic conditions. Diagenesis started with the dissolution of aragonite fans at the interface between single fans in non-laminated crusts and along lamination planes in isopachous, irregular, or crudely laminated crusts. Incomplete dissolution resulted in the development of secondary porosity within a matrix of undissolved aragonite fibers. Subsequently, the porosity was filled with calcite that systematically encased remaining aragonite crystals. This was followed by the dissolution of remnant aragonite fibers, producing a network of elongated inter- and intracrystalline pores that were eventually filled with low-Mg calcite. The stepwise substitution of fibrous aragonite by low-Mg calcite resulted in sparry, sparry-cloudy, sparry-micritic (including clotted micrite), and peloidal textures, which obscure the fibrous nature of the original deposits. Stable C- and O-isotope compositions suggest that early diagenesis was driven by meteoric and evaporative fluids. These observations unequivocally demonstrate destructive diagenesis, resulting in secondary textures, which mimic micritic and grumous (peloidal and clotted) textures associated with sparry microfabrics.

This suggests that these textures, classically interpreted as primary microbial precipitates and used as evidence of biogenicity in ancient microbialites, might be diagenetic products in some cases, even though at some stage, microbial processes and/or degradation of organic matter could have been involved in the diagenetic process.

1. Introduction

Carbonate seafloor precipitates include a range of mesofabrics, such as crystal fans, botryoids, radial fibrous microbotryoids, herringbone calcite, microdigitate stromatolites, and isopachous laminites (Grotzinger and Read, 1983; Grotzinger and Knoll, 1999; Grotzinger and James, 2000; Riding, 2008; Kah and Bartley, 2022). Seafloor precipitates comprise significant volumes of Precambrian laminated carbonates, especially in the Archean and Paleoproterozoic (Grotzinger, 1989; Sami and James, 1996; Sumner, 1997; Sumner and Grotzinger, 2000; Cantine et al., 2020). Their abundance decreased during the Mesoproterozoic except in restricted peritidal settings (Kah and Knoll, 1996; Bartley et al., 2000; Kah and Bartley, 2022), and were rare during the Neoproterozoic, except in the post-glacial cap carbonate facies (Corsetti and Lorentz, 2006; Hood and Wallace, 2018; Cantine et al., 2020). Seafloor carbonate precipitates also occur underlying Paleozoic evaporite deposits but became rarer during the Mesozoic and Cenozoic except for particular environmental conditions (Pope et al., 2000).

* Corresponding author at: Particle Vision GmbH, Passage du Cardinal 13B, Fribourg, Switzerland.
   E-mail address: david.jaramillo@particle-vision.ch (D. Jaramillo-Vogel).
   [1] Present address: TNO, Geological Survey of the Netherlands, Princetonlaan 6, Utrecht, the Netherlands.

Microbialites are organosedimentary deposits that have accreted as a result of the activity of a benthic microbial community (Burne and Moore, 1987). They include several types according to the mesostructure, the most common of which are stromatolites (laminated) and thrombolites (clotted) (Grey and Awramik, 2020 and references therein). Stromatolites are among the oldest evidence of biological activity on Earth, since their occurrence can be traced back to the Paleo-Archean (Walter et al., 1980; Lowe, 1980). They are common during the Paleoproterozoic, peak in abundance in the late Mesoproterozoic, and decline during the Neoproterozoic (Awramik, 1971; Hofmann, 1973; Grotzinger and James, 2000; Walter and Heys, 1985; Awramik and Sprinkle, 1999; Peters et al., 2017; Cantine et al., 2020). Thrombolites first occurred in the Paleoproterozoic and increased in abundance across the Proterozoic–Cambrian transition (Grotzinger and James, 2000; Cantine et al., 2020). Microbialite abundance in Phanerozoic marine deposits shows a decreasing trend with marked fluctuations from the Cambrian to Recent (Kiessling, 2002; Riding, 2005; Riding et al., 2019). Based on similarities with modern microbially-mediated carbonate deposits in fresh-water and marine environments (Aitken, 1967; Dupraz et al., 2009; Suosaari et al., 2016), fine-grained carbonate textures are considered distinctive evidence of a microbial-related origin of microbialites (Aitken, 1967; Grotzinger and Knoll, 1999; Riding, 2008, 2011; Riding and Virgone, 2020). According to Grey and Awramik (2020), microbialite microstructures made of fine-grained carbonate include micritic (structureless micrite), grumous (consisting of peloids and "clots that can be clumped together in an irregular manner"), granular (silt-sized particles), and tubular (tubes with micritic walls) textures. Microbialite microstructures also include microspar, which is considered to be the result of recrystallization of micritic calcite (Flügel, 2004; Grey and Awramik, 2020). In contrast, seafloor precipitates are considered essentially abiotic (i.e. precipitates in which biotic effects are negligible, Schlager, 2003; Riding and Virgone, 2020). Seafloor precipitates and microbialites can be intimately associated with hybrid carbonates (see Riding, 2008; Riding and Virgone, 2020), but are thought to reflect two distinct processes: abiotic and biologically mediated carbonate precipitation.

Here we show that diagenetic textures in essentially abiotic Pleistocene aragonite crusts of the Danakil Basin are strikingly convergent with fine-grained microtextures in ancient microbialites. The aragonite crusts formed during short intervals of increased carbonate saturation prior to evaporite precipitation during repeated episodes of isolation from the Red Sea (Atnafu et al., 2015; Jaramillo-Vogel et al., 2019).

2. Carbonate crusts in the Danakil Depression

Sedimentation in the Danakil Depression (Afar, Ethiopia) (Fig. 1A) was the result of the interaction between tectonics and eustatic sea-level changes that controlled connectivity with the Red Sea (Atnafu et al., 2015). The crusts occur at the top of two Pleistocene marine successions. These, termed the Lower and Upper successions and dated as MIS 7 and MIS 5e, respectively, record marine incursions into the Danakil Depression followed by desiccation (Fig. 1B) (Jaramillo-Vogel et al., 2019).

The oldest (MIS 7) aragonite crusts occur within and on top of coralline red algal frameworks that cap fringing coral reefs with normal-marine fauna (Fig. 1B). Coralline algal frameworks, up to 2 m in thickness, are laterally interfingered with shell-beds composed of the schizohaline bivalve *Brachidontes pharaonis* and gastropods, as well as oolites. The crusts are laminated, mamillar and columnar; they are often altered, and covered by an isopachous blocky calcite cement. The succession is covered by gypsum (Jaramillo-Vogel et al., 2019).

The younger crusts (MIS 5e; Fig. 1B) mainly form small irregular domes, centimeters to decimeters thick, on top of hard substrates, which may consist of coralgal deposits, bivalve concentrations, boulders or basement rocks. Crusts commonly have a columnar or non-columnar laminated appearance (up to 10 cm in thickness). Lamination within columns is flat to convex. Columns vary from coalesced non-branching to parallel branching with erect to recumbent morphologies. Columns, up to 6 cm in diameter, may be closely spaced or separated by sediment. Depending on the availability of hard substrate, crusts occur as isolated domes or cover extensive areas directly on the basement on steep, vertical and even overhanging walls. In deeper settings, down to 80 m paleodepth, crusts extend over the substrate with internal shrubby digitate structures (Jaramillo-Vogel et al., 2019). The crusts grew perpendicular to the substrate without any upward polarity (Jaramillo-Vogel et al., 2019).

The crusts in MIS 5e are laterally interfingered with shell-beds composed of the schizohaline bivalve *Brachidontes pharaonis* and gastropods, as well as oolites and spherulites. The spherulites are composed of single spherules made of radiating aragonite fibers. These spherules are associated with mobile substrates and were interpreted to have formed under the same environmental conditions as the crusts, but in the absence of a hard substrate (Jaramillo-Vogel et al., 2019).

The MIS 5e crusts are usually better preserved than those of MIS 7 and often retain their primary fibrous aragonite fabric. Some of these fibrous crusts contain Mg-silicates, that are interpreted to be a result of a microbial-mediated mineralization (Jaramillo-Vogel et al., 2019). These Mg-silicates are associated with non-laminated and irregularly laminated fabrics and are thus inferred to have formed by the interaction of microbial and abiotic precipitation, producing hybrid microbial/abiotic crusts (Jaramillo-Vogel et al., 2019).

Even though the occurrence of Mg-silicates in non-laminated and irregularly laminated fabrics suggests some degree of microbial-mediated mineralization, Jaramillo-Vogel et al. (2019) interpreted that most fibrous crusts in Afar are seafloor precipitates that formed due to supersaturated conditions prevailing after the closure of the connection to the Red Sea without significant microbial influence. This is especially the case for isopachous laminated fabrics. Microbes are present in
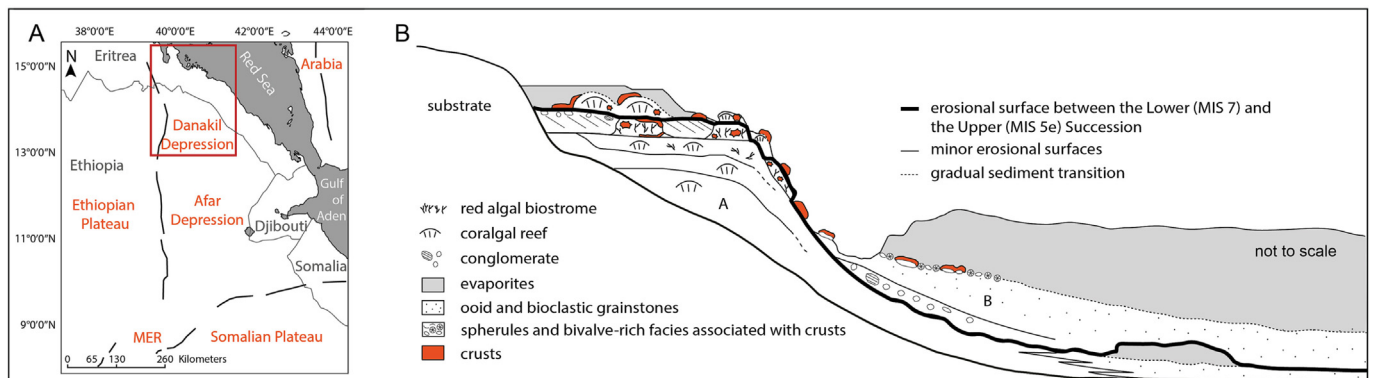

Fig. 1. A) Location of the study area (Danakil Depression, Afar, Ethiopia) and B) stratigraphic context of the fibrous aragonite crusts.
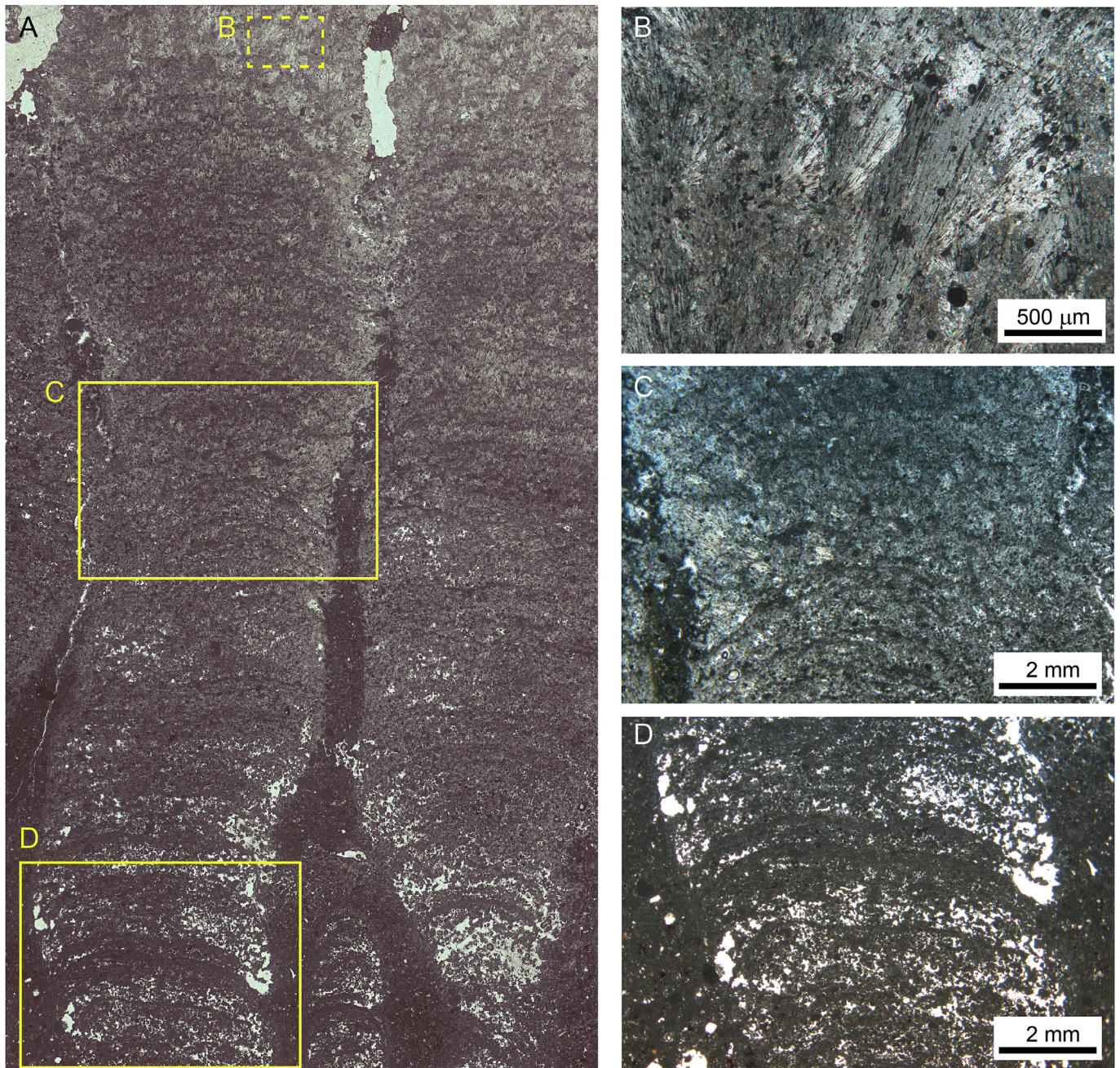(Modified after Jaramillo-Vogel et al. (2019).)

Fig. 2. A) Thin section scan of a crust showing the gradual facies change from an altered porous lower part made of micritic/peloidal laminae alternating with lamination-parallel porosity to a massive upper part made of aragonite fibers that show no clear lamination (the height of the image is about 4 cm). Images B to D represent zooms of the upper, middle and lower parts.

almost all environments on the Earth's surface, but the regularity and lateral continuity of the isopachous laminae imply a predominantly abiogenic origin for the lamination (Grotzinger, 1989; Grotzinger and Knoll, 1995; Pope et al., 2000; Riding, 2008, 2011).

Following gypsum precipitation, the MIS 7 crusts were subaerially exposed and then, depending on their location, some were re-flooded by marine waters and shared their subsequent evolution with MIS 5e crusts. The latter were covered by gypsum when the Danakil Depression was finally disconnected from the Red Sea and then subaerially exposed.

3. Methods

Descriptions of diagenetic fabrics on more than 50 thin sections were made with a standard petrographic microscope. The authors follow the definition of Flügel (2004) in which fabric includes both textural (shape, size, morphology, surface texture of individual grains) and structural components (orientation, arrangement in a rock). Twenty polished/freshly broken samples were coated with carbon and studied with a Zeiss GeminiSEM 300 scanning electron microscope at the Particle Vision GmbH laboratory (Fribourg, Switzerland). Stable carbon- and oxygen-isotope compositions of 18 micro-drilled carbonates of the altered facies were measured using a GasBench II (Thermo Fisher Scientific) linked to a Thermo Finnigan Delta Plus XL mass spectrometer at the Institute of Earth Surface Dynamics, University of Lausanne, Switzerland according to a method adopted after Spötl and Vennemann (2003). All results are reported in ‰ relative to the Vienna Pee Dee Belemnite standard (VPDB). The analytical reproducibility for three sequences was better than ± 0.06 ‰ for both $\delta^{13}C$ and $\delta^{18}O$ values for repeated measurements of the Carrara marble standard. Powder
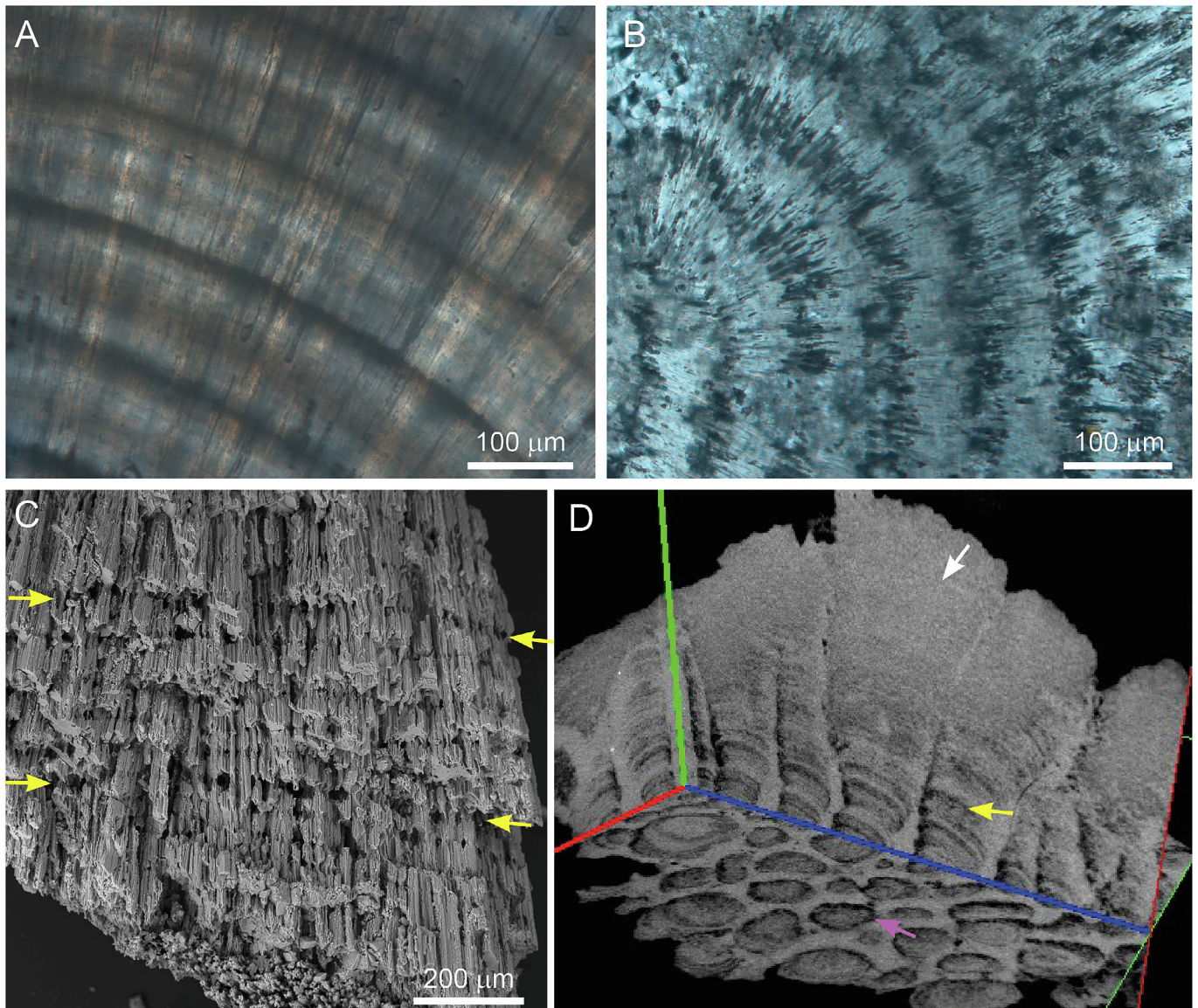
Fig. 3. A) Photomicrograph of a thin section showing an example of a pristine isopachous lamination inside an aragonite botryoid from a well-preserved crust. B) Thin section image showing isopachous laminated crust displaying initial dissolution along laminae (darker parts). C) SEM-SE image of a partially altered botryoid. Aragonite fibers are oriented from bottom to top. Note that fibers are sometimes interrupted by pores (black areas within the botryoid), and that these pores are dominantly arranged on planes perpendicular to the fibers (i.e. parallel to lamination planes; yellow arrows).

D) CT-image showing details of the three perpendicular planes of a reconstructed CT-scan of the partially altered crust shown in Fig. 2. The lighter gray values of the scan correspond to aragonite or calcite and the darker correspond to pores. The homogenous upper part (white arrow) is made of primary aragonite (see Fig. 2B) with no large porosity. The more altered lower part shows a clear lamination made of darker and brighter laminae composed of alternating diagenetic calcite (bright) and fenestral porosity (dark bands highlighted with the yellow arrow; see Fig. 2D). The basal plane shows that the crust is composed of discrete columns (purple arrow). Note that dissolution is strongest along lamination planes (dark bands) inside the columns. The sediment between the columns is less affected. The diameter of the columns is around 1 cm in the lower part.

samples for mineralogical analyses were extracted with a hand-held microdrill. Mineralogy was determined by X-ray diffractometry (XRD) at the Department of Geosciences (University of Fribourg) using a Rigaku Ultima IV diffractometer equipped with a D/teX detector (Rigaku Corporation, Tokyo, Japan) and a Cu X-ray tube operated at 40 kV and 40 mA.

X-ray tomography was performed using a multiscale nanotomograph "Bruker Skyscan2211" with a pixel resolution of 56 μm. Scanning mode was set on microfocus with a source voltage of 155 kV, current 35 μA, exposure time 1000 ms, rotation step 0.2° and frame averaging 4 as acquisition settings. Reconstruction was made with the software InstaRecon (Bruker) and visualization with DataViewer (Bruker).

Raman spectromicroscopy was performed on polished surfaces representing two different stages of diagenetic alteration. The analysis was

performed with a Witec alpha300 confocal Raman system (Witec GmbH, Germany) equipped with a green laser (532 nm) and coupled to a UHTS300 spectrometer with a grating of 600 g/mm, at the Gloor Instruments AG demo laboratory in the premises of Particle Vision GmbH in Fribourg. Raman spectra were acquired using a laser power of 20 mW. The map presented in Fig. 4E was acquired with a Zeiss EC Epiplan-Neofluer Dic 50×/0.8 objective, with an integration time of 0.05 s and a vertical and horizontal step size of 1.7 μm and 0.6 μm, respectively. The map shown in Fig. 6B was acquired with a Zeiss EC Epiplan-Neofluer Dic 100×/0.9 objective, with an integration time of 0.3 s and a vertical and horizontal step size of 0.12 μm. Spectral analysis was performed with the True Component Analysis tool of the Control SIX software (Witec GmbH, Germany).
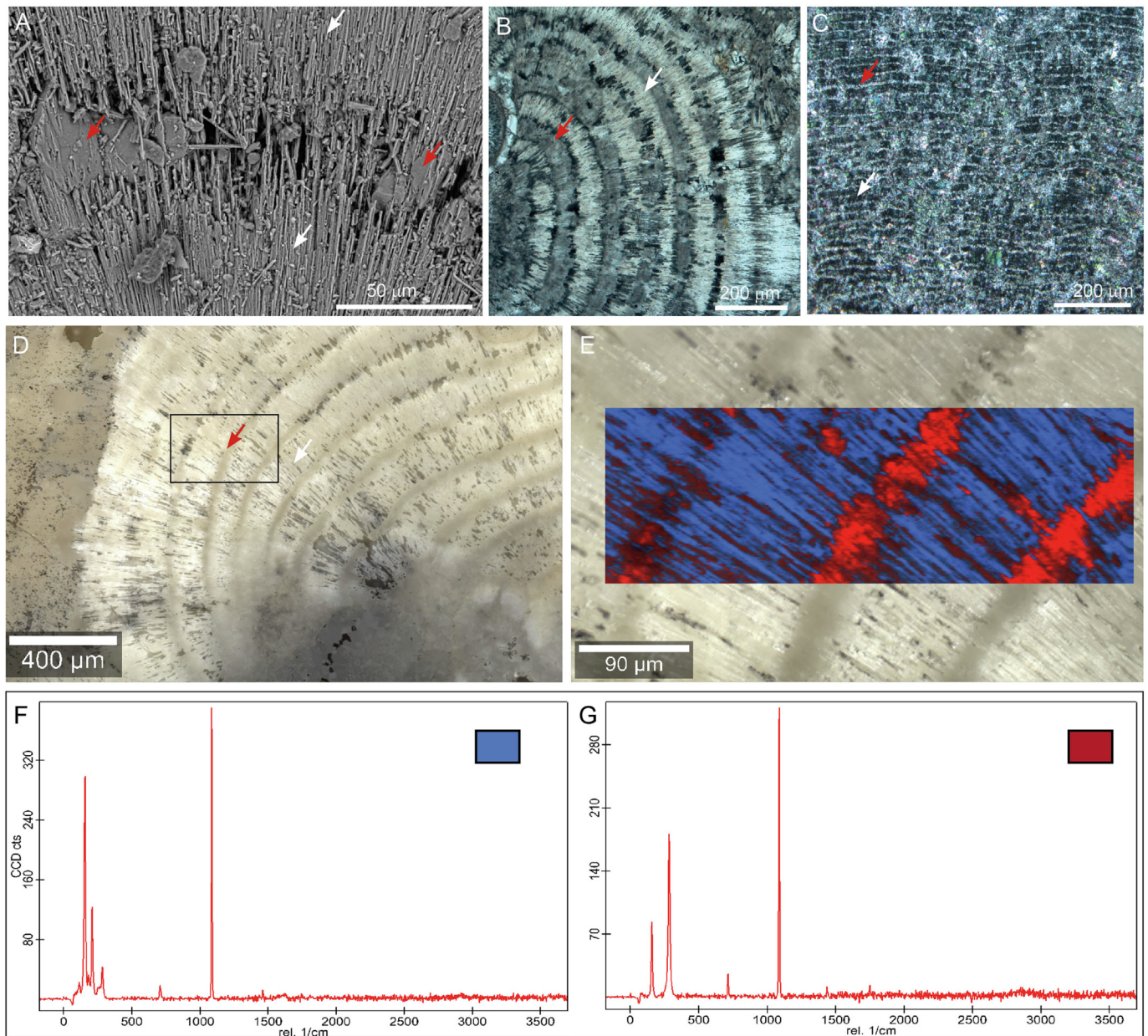
Fig. 4. A) SEM-SE image of a partly altered aragonite crust. Aragonite fibers are still present in the upper and lower part of the image (white arrows), while the central part shows secondary lamination parallel porosity that is partially filled with calcite crystals (red arrows). B) Alternation of primary aragonite fibers (white arrow) and secondary micritic/cloudy calcite (red arrow). C) Photomicrograph under crossed polars showing alternation of thicker primary aragonite (white arrow) and thinner secondary calcite laminae (red arrow) within former isopachous laminated crust. D) Overview of botryoidal aragonite showing thicker brighter laminae (white arrow) alternating with thinner darker laminae (red arrow). E) Raman map illustrates the alternation between aragonite (blue) and calcite (red) laminae (position shown by a square inset in D). F) Raman spectrum of aragonite (blue phase Raman map shown in E). G) Raman spectrum of calcite (the red phase Raman map shown in E).

4. Results

4.1. Diagenetic microfabrics

Pristine crusts consist of aragonite fibers forming isopachous laminated, irregular laminated and non-laminated fabrics (Jaramillo-Vogel et al., 2019). The lateral transition from unaltered fibrous aragonite to diagenetically modified fabrics can occur within a few centimeters (Fig. 2A, B, C, D). No single homogenous diagenetic product occurs, but rather a combination of secondary micrite, peloids, sparry-cloudy and sparry low-Mg calcite leading to sparry, clotted peloidal and associated sparry-micritic zones. We refer to "cloudy calcite" when it is darker than sparry calcite with no apparent micro-crystalline calcite.

The diagenetic substitution of fibrous aragonite occurs in discrete steps. In laminated fabrics, including both isopachous (Fig. 3A) and irregular laminated fabrics, diagenesis typically initiates along laminae (Fig. 3B). Further preferential dissolution of aragonite along lamination planes (Fig. 3C and D) results in laminated porosity. The newly created secondary porosity is filled by secondary cloudy calcite, micrite or sparite (Fig. 4A). This results in lamination consisting of the alternation between primary aragonite and secondary calcite (Fig. 4B–G). In non-laminated crusts, the dissolution of aragonite fans starts at the interface between single fans. At macro- to mesoscale, the alteration does not occur homogeneously throughout the crusts (Fig. 5A and B).

Additionally, in both laminated and non-laminated crusts, at the micro-crystalline scale, aragonite dissolution is seldom complete and
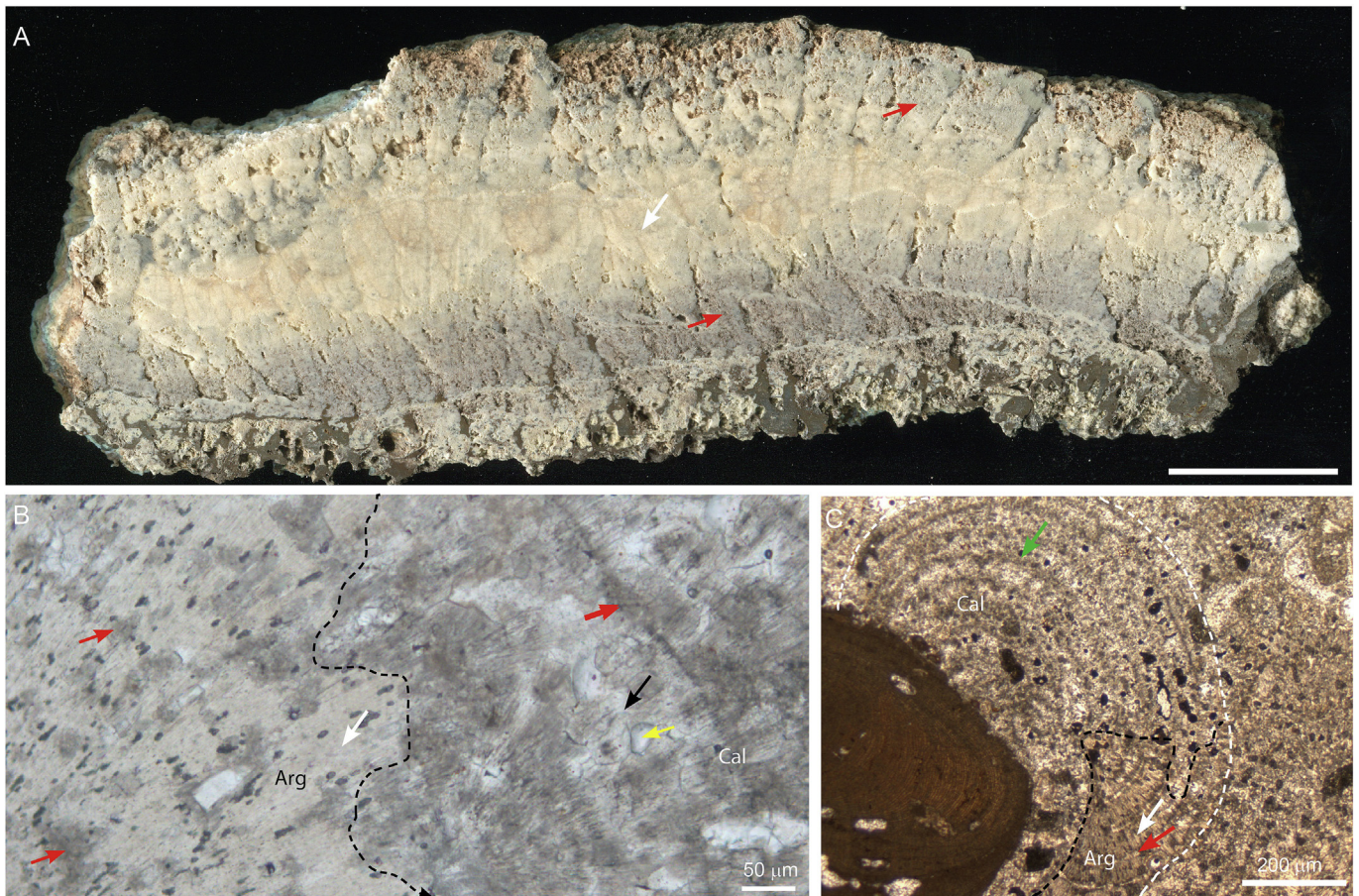
Fig. 5. A) Rock slab scan of a crust showing zones dominated by aragonite (white arrow) and calcite (red arrows), evidencing that alteration is not homogenous throughout the crust. B) Aragonite (Arg; white arrow) partly replaced by calcite (Cal) showing micritic/cloudy (red arrows) and more sparry (black arrow) laminae. The yellow arrow points to a pore. C) Botryoidal aragonite on red algae. Note that the lower part of the image shows an alternation of primary aragonite (white arrow) with secondary calcite (red arrow), while the upper part of the botryoid shows an alternation between micrite (green arrow) and sparitic calcite.

homogenous, affecting only part of the aragonite fibers (Fig. 5B and C). This results in zones where porosity coexists with loosely packed aragonite fibers. When calcite precipitates into the pores it typically incorporates loose relic aragonite fibers into the crystals (Fig. 6A and B). During this diagenetic step, aragonite can be present as dense fibrous aragonite (where little dissolution has occurred) as well as fibrous inclusion within the newly formed calcite cement (Fig. 4A, 6A). In some rare cases, microcrystalline calcite precipitates on the surface of partially dissolved aragonite fibers (Fig. 6C) prior to the precipitation of larger sparry calcite crystals.
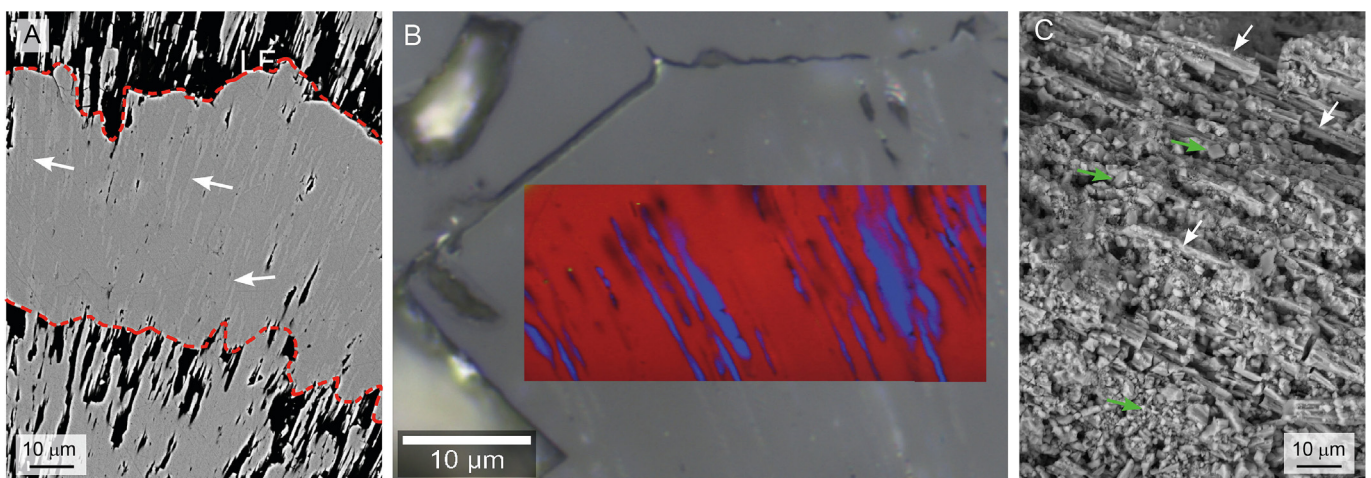

Fig. 6. A) Relict aragonite fibers (white arrows) enclosed in a large calcite crystal (SEM-BSD). Note that above and below the calcite crystal aragonite fibers are still present. B) Raman map of a calcite crystal (red on Raman map) with embedded aragonite fibers (blue on Raman map). C) SEM-SE image showing a cluster of microcrystalline calcite crystals (green arrows) growing in a partially dissolved aragonite crust. The aragonite fibers (white arrows) are largely covered by the micrite but in some places the fibrous morphology is still visible.
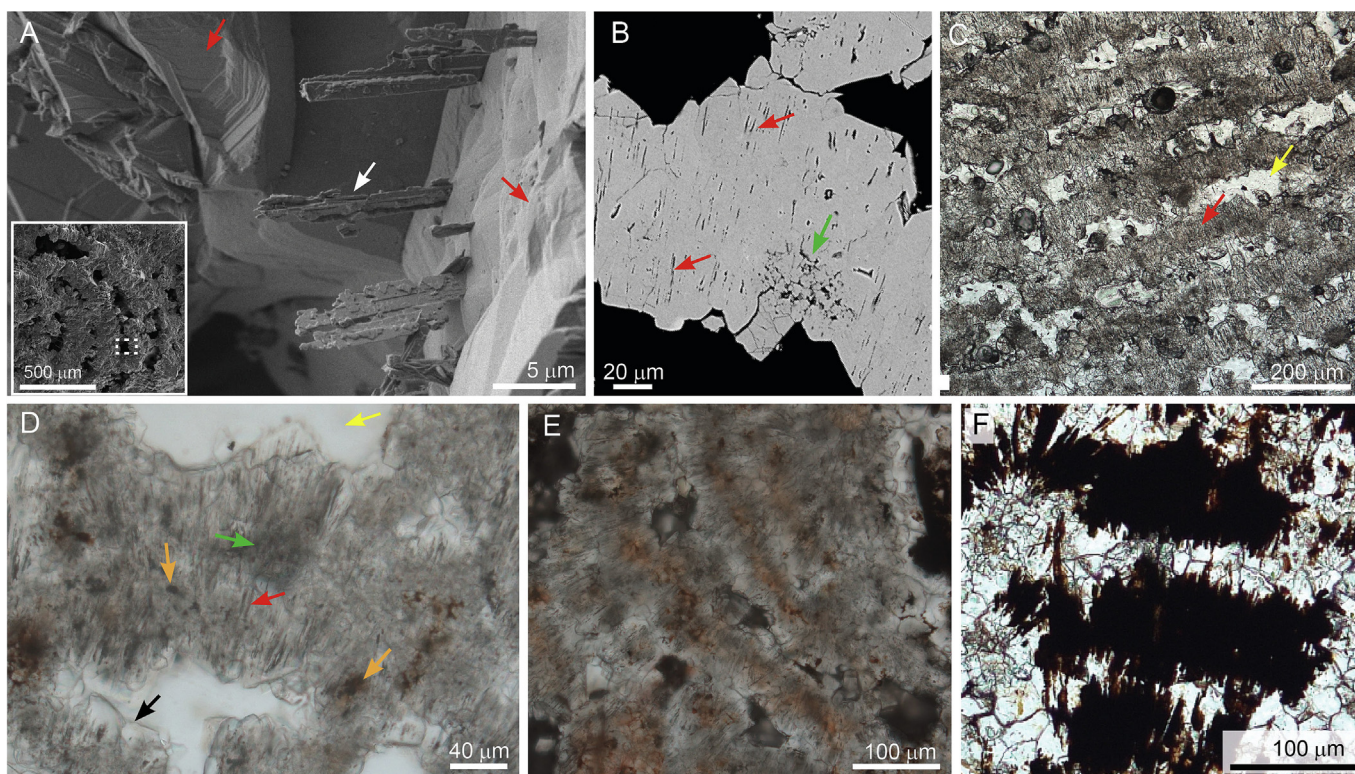
Fig. 7. A) SEM-SE image in the bottom left corner shows lamination-parallel porosity in an altered botryoid. Close up of one of the pores (square shows an approximate location) shows that after advanced dissolution a few altered aragonite fibers (white arrows) can still persist, indicating that dissolution can be incomplete. The hidden part of these protruding fibers is enclosed in secondary calcite (red arrow). B) Image showing elongated pores within calcite resulting from the dissolution of enclosed aragonite fibers (red arrows) and zones with micro-crystalline calcite (green arrow; micrite; SEM-BSD). C) Successive calcite laminae (red arrows) alternating with elongated pores (yellow arrow). D) Close up of altered fabric with sparry rims (black arrow), micritic zones (green arrow), elongated pores (red arrow), inclusions (orange arrows) and porosity (yellow arrow). The overall appearance of calcite is cloudy. E) Example of a lamination-parallel reddish micritic zone. This shows that the intracrystalline pores remaining after the dissolution of relict aragonite within the secondary calcite were connected, and that calcite precipitated within the pores is a different generation of calcite containing low amounts of oxides. F) Lamination-parallel precipitation of opaque material forming single fibers mimicking the morphology of the pores.

With progressing diagenesis, remnant aragonite fibers dissolve (Fig. 7A), resulting in the inversion of porosity and fabrics. Once the aragonite encased in calcite crystals dissolves, a network of elongated intracrystalline pores within the diagenetic calcite appears. In laminated fabrics, this results in rough lamination with relatively continuous laminae of calcite characterized by elongated intracrystalline pores perpendicular to lamination, alternating with irregular pores aligned parallel to lamination (Fig. 7B and C). The network of elongated intracrystalline pores within the calcite crystals can subsequently be filled by calcite and/or insoluble remnants, resulting in calcite with cloudy and micritic zones (Fig. 7D). These micritic zones sometimes show reddish colors (Fig. 7E) or contain opaque precipitations in the form of fibers following the morphology of the pore (Fig. 7F). Mg-silicates are rare in the diagenetically altered fabrics.

In a few cases, alteration results in peloidal fabrics (Fig. 8A), but more often, cloudy calcite and micrite fabrics occur together with sparry calcite (Fig. 8B). In this diagenetic process the characteristic fibrous aragonite disappears (Fig. 8C–F).

4.2. Stable carbon and oxygen isotopes

Stable isotopic values of well-preserved aragonitic crusts are similar throughout the various outcrops (Jaramillo-Vogel et al., 2019). Diagenetically modified fabrics, partially or fully composed of calcite, have lower $\delta^{13}C$ values (Fig. 9). Similar low values are noted for altered marine corals and bivalves in the same area (Fig. 9). Instead, no specific trend is apparent in $\delta^{18}O$ values. Alteration could lead to positive or negative shifts. Specific $\delta^{13}C$ and $\delta^{18}O$ values of altered fabrics differ depending on the outcrop. A vertical transect across a diagenetic front within one single crust (Fig. 10A and B) shows a decrease in $\delta^{13}C$ and an increase in $\delta^{18}O$ values with an increasing alteration.

5. Discussion

### 5.1. Origin of diagenetic microfabrics in the Danakil crusts

Differences in isotopic composition, depending on the outcrop, indicate that diagenesis was related to the local circulation of either meteoric and/or evaporative fluids. Small-scale primary porosity differences, physical crystal defects along irregularities (Frisia et al., 2002) and the presence of impurities such as Mg-silicates or organic matter, and its degradation (Jones, 2010; Pace et al., 2016), may influence the onset of localized $CaCO_3$ dissolution.

In Afar, alteration often starts with dissolution of aragonite, followed by calcite precipitation. However, there is no apparent link between the onset of aragonite dissolution and calcite precipitation. It is common to observe facies with lamination-parallel porosity but without secondary calcite. The first generation of calcite often produces micritic, cloudy or peloidal fabrics. These fabrics occur when aragonite fibers are incorporated into diagenetic calcite, which mostly happens during the early stages of diagenesis when the dissolution of aragonite is incomplete (Figs. 6A, 11A and B). Mg-silicates are associated with some fabrics in pristine crusts (Jaramillo-Vogel et al., 2019). However, remnant Mg-silicates are rare within the altered fabrics, as they were probably among the first phases to be dissolved. If associated with specific laminae, this could be one of the factors leading to preferential dissolution along lamination planes at an early stage of alteration. However, the present petrography cannot corroborate this assumption. It is also unknown to what extent the dissolved Mg-silicates possibly interact

within the rock to form the secondary fabrics. Thus, the role of Mg-silicates and other inhomogeneities inside the crust is not yet well understood and should be targeted in future studies.

Microcrystalline calcite precipitation within secondary pores and nested on aragonite fans has been described previously, for example,

in speleothems (Martín-García et al., 2009; Perrin et al., 2014). As demonstrated by Frisia et al. (2018) and Martín-Pérez et al. (2012), this phase of microcrystalline calcite can be interpreted as an early diagenetic product related to changes in hydrogeochemistry (Mg/Ca ratio, lake/brackish water influence, climate). According to Martín-García
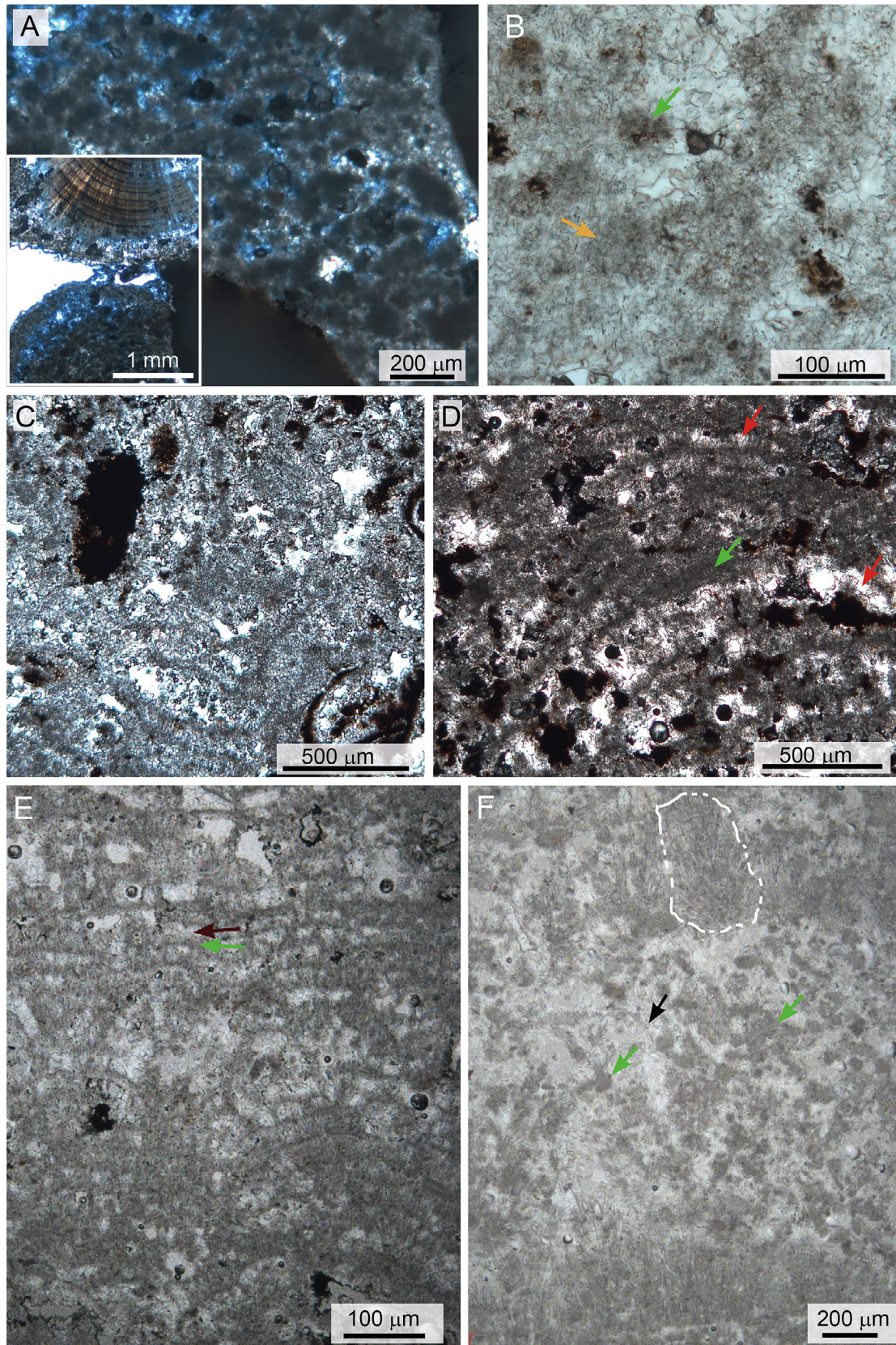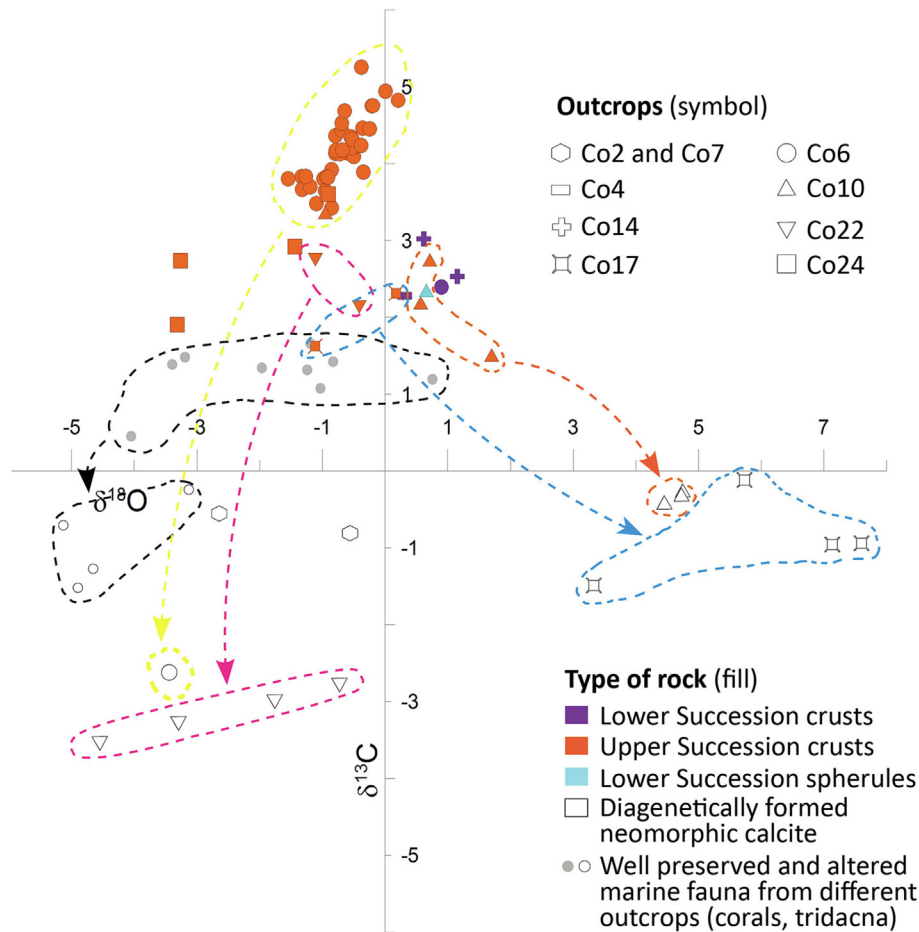
Fig. 9. Stable isotope compositions of well-preserved crusts and marine fauna (modified after Jaramillo-Vogel et al., 2019) with diagenetically altered counterparts. Arrows point toward altered counterparts, in the cases where both pristine and altered samples have been found in the same outcrop (except for the marine fauna). Altered crusts have lower C-isotope values but the O isotopic composition depends on the locality. Different symbols represent different localities.

et al. (2009) and Perrin et al. (2014), microcrystalline crystals in speleothems can act as nuclei for the growth of calcite mosaic crystals and progressive neomorphism (*sensu* Folk, 1965) of metastable arago-nite, eventually resulting in a mosaic of sparry calcite. Neomorphism may preserve relics of aragonite within the calcite as a result of only par-tial dissolution of the parent aragonite relative to newly precipitated secondary calcite (Aissaoui, 1985), as shown experimentally by Putnis and Putnis (2007) and Casella et al. (2017). Whereas the mechanisms inferred here (dissolution and then precipitation) are different from those invoked by these authors for speleothems (neomorphic re-placement), the onset of aragonite dissolution and subsequent cal-cite precipitation in the Afar crusts may have been driven similarly by changes in (local) hydrogeochemistry as inferred for speleothems (e.g. Mg/Ca, Sr/Ca ratio, evaporation, degassing). This is in line with the stable isotope compositional trends that suggest the involvement of me-teoric or evaporative fluids in aragonite crust alteration. At some places, the secondary calcite laminae are thicker than the original pore. This can be explained by small-scale replacement processes (coupled dissolution-precipitation steps) occurring at the pore walls, but this does not seem to be the dominant process.

Clusters of diagenetic microcrystalline calcite on partially dissolved aragonite fibers (Fig. 6C) have been observed and interpreted to have formed prior to the sparry calcite precipitation. These clusters most probably result in micritic or peloidal zones embedded within sparry calcite. However, these are local observations, and do not explain most of the observed diagenetic fabrics.

As diagenesis progresses, first non-enclosed (Fig. 11C) and later enclosed aragonite fibers dissolve (Figs. 7B, 11D), creating a network of elongated inter- and intracrystalline pores. The fact that reddish and opaque precipitates can be found along the laminae within the elongated pores (Fig. 7E and F) shows that these pores were connected.

Munnecke et al. (1997) described diagenetic processes occurring in an unconsolidated aragonite mud of Pliocene periplatform carbonates from a core retrieved in the Bahamas. The authors document calcite microspar precipitation encompassing aragonite needles, followed by the dissolution of aragonite in the microspar crystal leaving empty pits. They also argue that each aragonite needle had to be in contact with another constituent, to create a path for diagenetic fluids. This shows that aragonite can be first engulfed and subsequently dissolved during diagenesis of different types of sediments and under different

Fig. 8. Examples of altered microfabrics. A) Peloidal calcite (pores blue stained) replacing fibrous crust. Inset: partly preserved primary fibrous texture showing isopachous lamination of botryoidal aragonite from the same sample. B) Mixed cloudy (orange arrow) and micritic (green arrow) calcite embedded in sparry calcite. C) Non-laminated diagenetically altered fabric with peloid-like features and clotted fabric. Dark ellipses are serpulids. D) Irregular laminated fabric of micritic laminae (green arrow) intercalated with more sparry laminae (red arrow). E) Example of diagenetic alteration of formerly isopachous laminated fibrous facies. Lamination is made by the alternation of micritic/cloudy or peloidal (green arrow) and sparitic calcite laminae (black arrow). F) Non-laminated altered facies. This image shows peloids and micritic zones (green arrow) included in a sparry groundmass (black arrow). The zone marked with the white dashed line highlights a part of the crust where the previous fibrous nature is still recognizable.
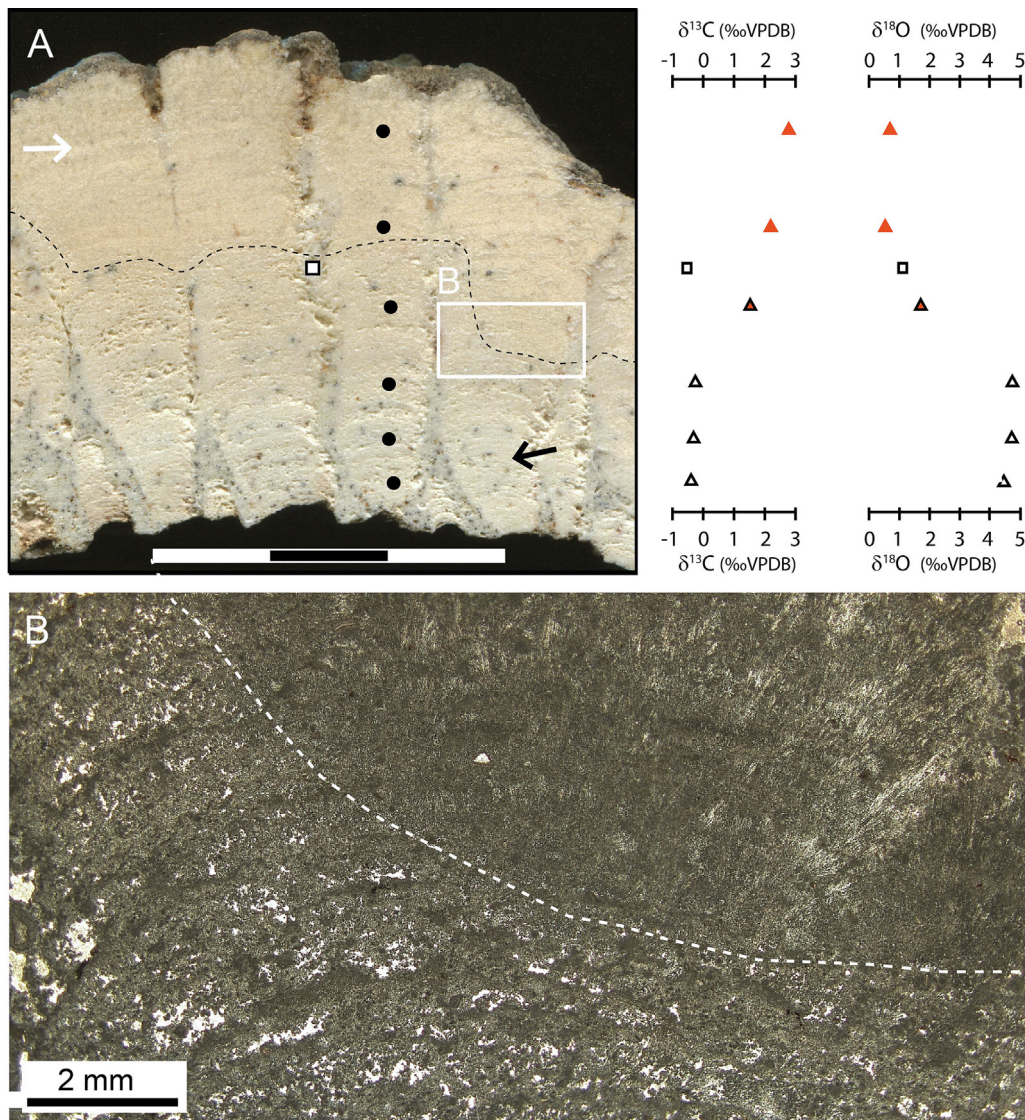
Fig. 10. A) Stable isotope transect through the transition from a well preserved zone composed of fibrous aragonite (white arrow) to an altered zone (black arrow) composed of calcite. White square is sediment between columns. B) Transition from well preserved crust (top right) to altered crust (left) showing fenestral porosity.

diagenetic conditions, suggesting that this could be a common path that can potentially have a strong transformational impact on primary fabrics.

The transformation of aragonite into calcite is also experimentally studied for aragonitic biominerals using hydrothermal fluids (80–175 °C) simulating the burial domain (Casella et al., 2017, 2018; Forjanes et al., 2022). These authors describe similarly a multi-step (neomorphic) replacement process with the formation and increase in secondary porosity during a first phase due to the dissolution of organic matter and/or biopolymers. This is subsequently followed by the dissolution of biogenic aragonite, and subsequent precipitation of abiogenic aragonite. Forjanes et al. (2022) evidence that the porosity network affects largely the kinetics of the alteration process. Also, for the Danakil crusts, the increase in secondary porosity may have influenced the reaction kinetics and circulation of meteoric fluids along lamination planes.

Although the link with the enclosed aragonite is evident and believed to be the crucial condition for the large-scale facies transformations, the exact timing and geochemical processes related to the formation of cloudy and micritic calcite within the calcite crystals are unclear. One hypothesis is that the pore network results in enlarged reactive surfaces where different processes leading to cloudy and micritic fabrics occur. As these processes occur at microscale, it is however,

necessary to perform targeted experiments specially designed to detangle these processes. Another hypothesis is that small insoluble remnants or precipitates (such as oxides or Mg-silicates) provide nucleation sites within the pores, which may lead to micrite precipitation. These remnants, together with the newly created micrite, could be responsible for the formation of micritic zones within the sparry calcite crystals (Fig. 11E2, E3). During later diagenesis, when the aragonite is fully dissolved, calcite precipitates into empty pores forming sparry calcite.

When cloudy and micritic zones are embedded in sparry calcite (Figs. 8A–F, 11E), they form diagenetic fabrics that are similar to true microbial microcrystalline and peloidal fabrics. With advancing diagenesis, cloudy and micritic facies converge, making it difficult to recognize them as altered aragonite fabrics. The fact that both isopachous laminated and non-laminated crusts can give rise to irregular, cloudy, clotted micritic and peloidal fabrics, emphasizes that different primary textures can progressively converge during diagenesis (Della Porta, 2015; De Boever et al., 2017).

5.2. Fine-grained microfabrics as biogenicity criteria

The altered aragonite-crust fabrics in Afar suggest that, in some cases, fine-grained textures in ancient stromatolites, and thrombolites might
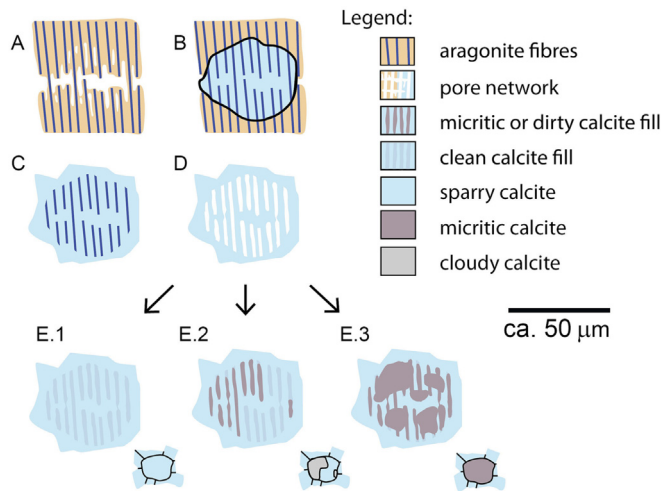
Fig. 11. Microfabric alteration leading to cloudy, micritic and peloid fabric formation. A) Incomplete aragonite dissolution along laminae. B) Calcite precipitates filling pores including aragonite fibers and other undissolved remnants within crystals. At this step replacement (coupled dissolution-precipitation) may occur. C) Aragonite dissolution continues while calcite crystals continue to grow. D) Aragonite fibers within calcite crystals are eventually dissolved and new pores appear. E) Possible pathways after aragonite dissolution and resulting microfacies (lower right). E.1) Precipitation of clean calcite within pores preserves sparry nature. E.2) Precipitation of calcite with oxides or other impurities or the deposition of insoluble remnants occurring together with clean sparry calcite is interpreted to results in cloudy calcite. E.3) Micritic zones form within calcite crystals resulting in micritic fabric. The link with the first enclosed and then dissolved aragonite is evident and believed to be the crucial condition, however, the timing and geochemical processes related to micritic calcite formation within the calcite crystals are unclear. Primary dissolution-pores form a template for the formation of micritic features. Depending on the continuity of primary dissolution-pores shown in step A, calcite precipitation forms elongated cloudy or micritic laminae, or isolated cloudy spots, or peloids. Microcrystalline calcite has been observed to locally form clusters inside the pores. Although these clusters have the potential to form micritic and peloidal zones, these are not responsible for most of the diagenetic fabrics. Therefore, they are not included in the drawings.

not reflect a direct biogenic origin. Micrite and grumous textures, and in general fine-grained textures, are considered indicative of a microbial origin of ancient stromatolites, thrombolites and other microbial carbonates (Riding, 2000, 2011; Grey and Awramik, 2020, and references therein). In the Pleistocene of Afar, however, these textures are the result of diagenetic alteration of seafloor precipitates. Grumous microstructure/texture is composed of peloids and clots/grumeaux (patches of micrite with diffuse boundaries that grade into surrounding microsparite; Turner et al., 2000), which can be clumped together. This texture, also referred to as clotted fabric (Riding, 2000), is common in stromatolites and thrombolites, from Proterozoic microbial carbonates (Riding and Sharma, 1998) up to Recent examples (Dupraz et al., 2009; Suosaari et al., 2016). Fine-grained textures occur intimately associated with sparry carbonate in many of Archean and Proterozoic stromatolites (Riding, 2008, 2011; Riding and Virgone, 2020). They are referred to as ribboned and striated (Hoffman, 1969), streaky (Walter, 1972), filmy (Knoll and Semikhatov, 1998), spar-micrite couplets (Sami and James, 1996) or hybrid crusts (Riding, 2008, 2011; Riding and Virgone, 2020). Hybrid crusts are known from the Archean and may have been the dominant fabrics in Paleo- and Mesoproterozoic stromatolites (Riding, 2011). The fine-grained components are assumed to reflect a biotic origin, which is combined to varying degrees with abiotic seafloor precipitation to build the crust (Grotzinger and Knoll, 1999; Sami and James, 1996; Kah and Riding, 2007). Based on our observations, at least in some cases, fine-grained fabrics in hybrid crusts and in other carbonates interpreted as microbial could result from diagenetic alteration of original fibrous, essentially abiotic, crystalline crusts. For the Afar crusts, the impurities associated with the nucleation of microcrystalline calcite could arguably be organic (e.g. insoluble organic residues, Mg-silicates), and, therefore, the micritic fabrics could be of

indirect microbial origin. It is important, however, to keep in mind that these fabrics are diagenetic features.

6. Conclusions

Irrespective of the type of fibrous crust (isopachous laminated, irregularly laminated and non-laminated), diagenesis of fibrous aragonite fabrics in the Danakil Depression (Afar, Ethiopia) led to secondary sparry, micritic, and clotted peloidal calcite fabrics, traditionally considered to be indicative of a biotic origin. Due to the stepwise replacement of aragonite by calcite, lamination can be preserved, even enhanced, while the fibrous fabrics disappear.

The formation of these fabrics is interpreted to be mainly driven by the encasement of partially dissolved aragonite fibers in sparry calcite and the later dissolution, that creates a network of elongated pores. It is interpreted that the pore network results in enlarged reactive surfaces, where the different processes linked to precipitation of calcite and other minerals, occur. In this context, insoluble remnants or precipitates (such as oxides or Mg-silicates) could also play a role by providing nucleation sites that can lead to micrite precipitation. However, the timing and geochemical processes related to micrite formation within the calcite crystals are still unclear.

Pre-evaporitic environmental settings similar to those during the Danakil crust formation may have been common for stromatolites since the Paleoproterozoic (Pope et al., 2000), making it likely that some laminated-carbonate formations since then have followed diagenetic pathways comparable to those studied here. Fine-grained microfabrics of ancient stromatolites and thrombolites should be interpreted carefully as they could be abiotic diagenetic products.

References

Aissaoui, D.M., 1985. Botryoidal aragonite and its diagenesis. Sedimentology 32, 345–361.
Aitken, J.D., 1967. Classification and environmental significance of cryptalgal limestones and dolomites, with illustrations from the Cambrian and Ordovician of southwestern Alberta. Journal of Sedimentary Petrology 37, 1163–1178.

Atnafu, B., Kidane, T., Foubert, A., Jaramillo-Vogel, D., Schaegis, J.-C., Henriet, J.-P., 2015. Reading history in Afar. EOS 96, 12–15.

Awramik, S.M., 1971. Precambrian columnar stromatolite diversity: reflection of metazoan appearance. Science 174, 825–827.

Awramik, S.M., Sprinkle, J., 1999. Proterozoic stromatolites: the first marine evolutionary biota. Historical Biology 13, 241–253.

Bartley, J.K., Knoll, A.H., Grotzinger, J.P., Sergeev, V.N., 2000. Lithification and fabric genesis in precipitated stromatolites and associated peritidal carbonates, Mesoproterozoic Billyakh Group, Siberia. In: Grotzinger, J.P., James, N.P. (Eds.), Carbonate Sedimentation and Diagenesis in the Evolving Precambrian World. SEPM Special Publicationvol. 67. SEPM, Tulsa, pp. 60–73.

Burne, R.V., Moore, L.S., 1987. Microbialites: organosedimentary deposits of benthic microbial communities. Palaios 2, 241–245.

Cantine, M.D., Knoll, A.H., Bergmann, K.D., 2020. Carbonates before skeletons: a database approach. Earth-Science Reviews 201, 103065. https://doi.org/10.1016/j.earscirev.2019.103065.

Casella, L.A., Griesshaber, E., Yin, X., Ziegler, A., Mavromatis, V., Müller, D., Ritter, A.C., Hippler, D., Harper, E.M., Dietzel, M., Immenhauser, A., Schöne, B.R., Angiolini, L., Schmahl, W.W., 2017. Experimental diagenesis: Insights into aragonite to calcite transformation of *Arctica islandica* shells by hydrothermal treatment. Biogeosciences 14, 1461–1492. https://doi.org/10.5194/bg-14-1461-2017.

Casella, L.A., He, S., Griesshaber, E., Fernández-Díaz, L., Greiner, M., Harper, E.M., Jackson, J. J., Ziegler, A., Mavromatis, V., Dietzel, M., Eisenhauer, A., Veintemillas-Verdaguer, S., Brand, U., Schmahl, W.W., 2018. Hydrothermal alteration of aragonitic biocarbonates: assessment of micro-and nanostructural dissolution–reprecipitation and constraints of diagenetic overprint from quantitative statistical grain-area analysis. Biogeosciences 15 (24), 7451–7484.

Corsetti, F.A., Lorentz, N.J., 2006. On Neoproterozoic cap carbonates as chronostratigraphic markers. In: Xiao, S., Kaufman, A.J. (Eds.), Neoproterozoic Geobiology and Paleobiology. Springer, Dordrecht, pp. 273–294.

De Boever, E., Brasier, A.T.A.T., Foubert, A., Kele, S., 2017. What do we really know about early diagenesis of non-marine carbonates? Sedimentary Geology 361, 25–51.

Della Porta, G., 2015. Carbonate build-ups in lacustrine, hydrothermal and fluvial settings: comparing depositional geometry, fabric types and geochemical signature. Geological Society of London, Special Publication 418, SP418–4 (London).

Dupraz, C., Reid, R.P., Braissant, O., Decho, A.W., Norman, R.S., Visscher, P.T., 2009. Processes of carbonate precipitation in modern microbial mats. Earth-Science Reviews 96, 141–162.

Flügel, E., 2004. Microfacies of Carbonate Rocks. Springer, Berlin, Heidelberg (976 pp.).

Folk, R.L., 1965. Petrology of Sedimentary Rocks. Hemphill Publishing Company, Austin, Texas, p. 78703.

Forjanes, P., Simonet Roda, M., Greiner, M., Griesshaber, E., Lagos, N.A., Veintemillas-Verdaguer, S., Astilleros, J.M., Fernandez-Diaz, L., Schmahl, W.W., 2022. Experimental burial diagenesis of aragonitic biocarbonates: from organic matter loss to abiogenic calcite formation. Biogeosciences 19 (16), 3791–3823.

Frisia, S., Borsato, A., Fairchild, I.J., Mcdermott, F., Selmo, E.M., 2002. Aragonite–calcite relationships in speleothems (Grotte De Clamouse, France): environment, fabrics, and carbonate geochemistry. Journal of Sedimentary Research 72, 687–699.

Frisia, S., Borsato, A., Hellstrom, J., 2018. High spatial resolution investigation of nucleation, growth and early diagenesis in speleothems as exemplar for sedimentary carbonates. Earth-Science Reviews 178, 68–91.

Grey, K., Awramik, S.M., 2020. Handbook for the study and description of microbialites. GSWA Bulletin 147 (279 pp.).

Grotzinger, J.P., 1989. Facies and evolution of Precambrian carbonate depositional systems: emergence of the modem platform archetype. In: Crevello, P.D., Wilson, J.L., Sarg, J.E., Read, J.E. (Eds.), Controls on Carbonate Platform and Basin Development. SEPM Spec. Publ.vol. 44. SEPM, Tulsa, pp. 79–106.

Grotzinger, J.P., James, N.P., 2000. Precambrian carbonates: evolution of understanding. In: Grotzinger, J.P., James, N.P. (Eds.), Carbonate Sedimentation and Diagenesis in the Evolving Precambrian World. SEPM Special Publicationvol. 67. SEPM, Tulsa, pp. 3–20.

Grotzinger, J.P., Knoll, A.H., 1995. Anomalous carbonate precipitates: is the Precambrian the key to the Permian? Palaios 10, 578–596.

Grotzinger, J.P., Knoll, A.H., 1999. Stromatolites in Precambrian carbonates: evolutionary mileposts or environmental dipsticks? Annual Review of Earth and Planetary Sciences 27, 313–358.

Grotzinger, J.P., Read, J.F., 1983. Evidence for primary aragonite precipitation, lower Proterozoic (1.9-Ga) Rocknest Dolomite, Wopmay Orogen, Northwest Canada. Geology 11, 710–713.

Hoffman, P.F., 1969. Proterozoic paleocurrents and depositional history of the East Arm Fold Belt, Great Slave Lake, Northwest Territories. Canadian Journal of Earth Sciences 6, 441–462.

Hofmann, H.J., 1973. Stromatolites: characteristics and utility. Earth-Science Reviews 9, 339–373.

Hood, A.v.S., Wallace, M.W., 2018. Neoproterozoic marine carbonates and their paleoceanographic significance. Global and Planetary Change 160, 28–45.

Jaramillo-Vogel, D., Foubert, A., Braga, J.C., Schaegis, J.C., Atnafu, B., Grobety, B., Kidane, T., 2019. Pleistocene seafloor fibrous crusts and spherulites in the Danakil Depression (Afar, Ethiopia). Sedimentology 66, 480–512.

Jones, B., 2010. Microbes in caves: agens of calcite corrosion and precipitation. In: Pedley, H.M., Rogerson, M. (Eds.), Tufas and Speleothems: Unravelling the Microbial and Physical Controls. Geological Society of London, Special Publication No. 336, pp. 7–30.

Kah, L.C., Bartley, J.K., 2022. Carbonate fabric diversity and environmental heterogeneity in the late Mesoproterozoic Era. Geological Magazine 159, 220–246. https://doi.org/10.1017/S0016756821000406.

Kah, L.C., Knoll, A.H., 1996. Microbenthic distribution of Proterozoic tidal flats: environmental and taphonomic considerations. Geology 24, 79–82.

Kah, L.C., Riding, R., 2007. Mesoproterozoic carbon dioxide levels inferred from calcified cyanobacteria. Geology 35, 799–802.

Kiessling, W., 2002. Secular variations in the Phanerozoic reef ecosystem. In: Kiessling, W., Flügel, E., Golonka, J. (Eds.), Phanerozoic Reef Patterns. SEPM Special Publicationvol. 72. SEPM, Tulsa, pp. 625–690.

Knoll, A.H., Semikhatov, M.A., 1998. The genesis and time distribution of two distinctive Proterozoic stromatolite microstructures. Palaios 13, 408–422.

Lowe, D.R., 1980. Stromatolites 3,400–3,500 Myr old from the Archean of Western Australia. Nature 284, 441–443.

Martín-García, R., Alonso-Zarza, A.M., Martín-Pérez, A., 2009. Loss of primary texture and geochemical signatures in speleothems due to diagenesis: Evidences from Castañar Cave, Spain. Sedimentary Geology 221, 141–149.

Martín-Pérez, A., Martín-García, R., Alonso-Zarza, A.M., 2012. Diagenesis of a drapery speleothem from Castañar Cave: from dissolution to dolomitization. International Journal of Speleology 41, 251–266.

Munnecke, A., Westphal, H., Reijmer, J.J., Samtleben, C., 1997. Microspar development during early marine burial diagenesis: a comparison of Pliocene carbonates from the Bahamas with Silurian limestones from Gotland (Sweden). Sedimentology 44 (6), 977–990.

Pace, A., Bourillot, R., Bouton, A., Vennin, E., Galaup, S., Bundeleva, I., Patrier, P., Dupraz, C., Thomazo, C., Sansjofre, P., Yokoyama, Y., Franceschi, M., Anguy, Y., Pigot, L., Virgone, A., Visscher, P.T., 2016. Microbial and diagenetic steps leading to the mineralisation of Great Salt Lake microbialites. Scientific Reports 6, 31495.

Perrin, C., Prestimonaco, L., Servelle, G., Tilhac, R., Maury, M., Cabrol, P., 2014. Aragonite-calcite speleothems: identifying original and diagenetic features. Journal of Sedimentary Research 84, 245–269.

Peters, S.E., Husson, J.M., Wilcots, J., 2017. The rise and fall of stromatolites in shallow marine environments. Geology 45, 487–490.

Pope, M.C., Grotzinger, J.P., Schreiber, B.C., 2000. Evaporitic subtidal stromatolites produced by in situ precipitation: textures, facies associations, and temporal significance. Journal of Sedimentary Research 70 (5), 1139–1151.

Putnis, A., Putnis, C.V., 2007. The mechanism of re-equilibration of solids in the presence of a fluid phase. Journal of Solid State Chemistry 180, 1783–1786.

Riding, R., 2000. Microbial carbonates: the geological record of calcified bacterial-algal mats and biofilms. Sedimentology 47, 179–214. https://doi.org/10.1046/j.1365-3091.2000.00003.x.

Riding, R., 2005. Phanerozoic reefal microbial carbonate abundance: comparisons with metazoan diversity, mass extinction events, and seawater saturation state. Revista Española de Micropaleontología 37, 23–39.

Riding, R., 2008. Abiogenic, microbial and hybrid authigenic carbonate crusts: components of Precambrian stromatolites. Geologia Croatica 61 (2–3), 73–103.

Riding, R., 2011. The nature of stromatolites: 3,500 million years of history and a century of research. In: Reitner, J., Quéric, N.-V., Arp, G. (Eds.), Advances in Stromatolite Geobiology. Springer, Berlin Heidelberg, pp. 29–74.

Riding, R., Sharma, M., 1998. Late Palaeoproterozoic (~1800–1600 Ma) stromatolites, Cuddapah Basin, southern India: cyanobacterial or other bacterial microfabrics? Precambrian Research 92, 21–35.

Riding, R., Virgone, A., 2020. Hybrid Carbonates: in situ abiotic, microbial and skeletal co-precipitates. Earth-Science Reviews 208, 103300. https://doi.org/10.1016/j.earscirev.2020.103300.

Riding, R., Liang, L., Lee, J.-H., Virgone, A., 2019. Influence of dissolved oxygen on secular patterns of marine microbial carbonate abundance during the past 490 Myr. Palaeogeography, Palaeoclimatology, Palaeoecology 514, 135–143.

Sami, T.T., James, N.P., 1996. Synsedimentary cements as Paleoproterozoic platform building blocks, Pethei Group, northwestern Canada. Journal of Sedimentary Research 66, 209–222.

Schlager, W., 2003. Benthic carbonate factories of the Phanerozoic. International Journal of Earth Sciences 92, 445–464.

Spötl, C., Vennemann, T.W., 2003. Continuous-flow IRMS analysis of carbonate minerals. Rapid Communications in Mass Spectrometry 17, 1004–1006.

Sumner, D.Y., 1997. Carbonate precipitation and oxygen stratification in Late Archean seawater as deduced from facies and stratigraphy of the Gamohaan and Frisco formations, Transvaal Supergroup. South Africa. American Journal of Science 297, 455–487.

Sumner, D.Y., Grotzinger, J.P., 2000. Late Archean aragonite precipitation: petrography, facies associations, and environmental significance. In: Grotzinger, J.P., James, N.P. (Eds.), Carbonate Sedimentation and Diagenesis in the Evolving Precambrian World. SEPM Special Publicationvol. 67. SEPM, Tulsa, pp. 123–144.

Suosaari, E.P., Reid, R.P., Playford, P.E., Foster, J.S., Stolz, J.F., Casaburi, G., Hagan, P.D., Chirayath, V., Macintyre, I.G., Planavsky, N.J., Eberli, G.P., 2016. New multiscale perspectives on the stromatolites of Shark Bay, Western Australia. Scientific Reports 6, 20557.

Turner, E.C., James, N.P., Narbonne, G.M., 2000. Taphonomic control on microstructure in early Neoproterozoic reefal stromatolites and thrombolites. Palaios 15, 87–111.

Walter, M.R., 1972. Stromatolites and the biostratigraphy of the Australian Precambrian and Cambrian. Special Papers in Palaeontology 11, 1–190.

Walter, M.R., Heys, G.R., 1985. Links between the rise of the Metazoa and the decline of stromatolites. Precambrian Research 29, 149–174.

Walter, M.R., Buick, R., Dunlop, J.S.R., 1980. Stromatolites 3,400–3,500 Myr old from the North Pole area, Western Australia. Nature 284, 443–445.